

## Investigation on resonant laser ablation spectrum of Fe in 281.5–285.5 nm wavelength region

MA JING<sup>1\*</sup>, JI XUEHAN<sup>2</sup>, CUI ZHIFENG<sup>2</sup>

<sup>1</sup>Department of Electronic Science and Applied Physics, College of Physics and Information Engineering, Fuzhou University, Fujian Fuzhou, 350002, P.R. China

<sup>2</sup>Laboratory of Atomic and Molecular Physics, Department of Physics, Anhui Normal University, Anhui Wuhu, 24100, P.R.China

\*Corresponding author: majing@fzu.edu.cn

Laser ablation of solid Ti samples has been studied using a tunable pulsed dye laser. Six resonant laser ablation (RLA) spectral lines of Fe in the Ti sample are firstly measured in the 281.5–285.5 nm wavelength region. The initial state of the RLA spectral lines is  $a^5F$ , the resonant states are  $z^5H^0$ ,  $x^5P^0$  and  $y^5G^0$ , respectively. The influence of laser power density on the intensities of RLA spectrum is discussed. The relationship between the laser wavelength and the photo-ionization cross sections of the resonant state  $^5G^0$  is analyzed.

Keywords: resonant laser ablation (RLA), resonant state, photo-ionization cross section.

### 1. Introduction

Resonant laser ablation (RLA) is a two-step process, occurring within a tunable laser, in which the leading edge of laser pulse ablates the surface of the solid sample to produce neutral atoms or molecules that are resonantly ionized by the trailing edge of the same pulse. Nowadays RLA is rapid gaining popularity as a method of sample introduction for mass spectrometry and it provides a useful sampling mechanism for chemical analysis [1–12]. BORTHWICK *et al.* [3] studied Fe element by RLA technique. 307.66 nm and 308.46 nm RLA spectral lines of Fe were measured by mass spectrum. The initial state of these two spectral lines is  $^5F$  and the resonant state is  $^5D^0$ . EIDEN and NOGAR [4] studied the two-photon spectrum of Fe by RLA. The initial states of the RLA spectral lines of Fe are  $a^5F$ ,  $a^5D$  and  $a^3F$ , respectively. The resonant states are  $e^5D$ ,  $e^5F$ ,  $e^5P$  and  $g^5D$ , respectively. In this paper, six RLA spectral lines of Fe are firstly measured in 281.5–285.5 nm wavelength region. The initial state of the RLA spectral lines is  $a^5F$ , the resonant states are  $z^5H^0$ ,  $x^5P^0$  and  $y^5G^0$ ,

respectively. Experiment results show that there is a proportional relation between the photo-ionization cross section of  $y^5G^0$  resonant state and the laser wavelength. The influence of laser power density on the intensity of RLA spectrum has also been discussed.

## 2. Experimental

The experimental setup is shown in Fig. 1. The laser arrangement consisted of a Nd:YAG laser (Spectra-Physics, LAB 170, 532 nm) and a pumping tunable dye laser (Sirah, PRSC-D-30) employing Rhodamine 6G. The dye laser output was frequency doubled by KDP crystal with 10 Hz repetition rate and pulse length less than 10 ns. The laser beam was focused by quartz lens ( $f = 25$  cm) to give a beam diameter of 0.5 mm. The laser intensity onto the surface of the sample was typically  $10^7$  Wcm<sup>-2</sup>. The sample was placed between two electrodes which were separated by 1 cm. 300VDC potential was applied to the upper electrode to serve as an ion repeller. The lower electrode was grounded through a load resistor to serve as an ion collector. The electrodes were placed in a stainless steel chamber which was pumped by a mechanical pump. Ion signal averaged by a boxcar integrator (Stanford Research Systems, SR250 and SR245) was sent to a computer for storage and subsequent data analysis.

## 3. Results and discussion

The sample used in our experiment was Ti sample (99.7%). The content of Fe was 0.12%. The RLA spectrum obtained from the Ti sample at the wavelength region from 281.5 nm to 285.5 nm was shown in Fig. 2. Six spectral lines were assigned as the atomic transition of Fe. The energy levels of the participating states for every line were 282.99 nm ( $a^5F_2 \rightarrow z^5H_3^0$ ), 284.96 nm ( $a^5F_2 \rightarrow x^5P_1^0$ ), 282.45 nm ( $a^5F_3 \rightarrow y^5G_3^0$ ), 283.39 nm ( $a^5F_3 \rightarrow y^5G_4^0$ ), 283.93 nm ( $a^5F_2 \rightarrow y^5G_2^0$ ) and 284.40 nm ( $a^5F_2 \rightarrow y^5G_3^0$ ), respectively.

The (1+1) resonant ionization processes corresponding with the six RLA spectral lines of Fe were shown in Fig. 3. The RLA spectral lines of Fe were produced from the transitions of fine structure of the same electronic state  $a^5F$  as initial state to three different electronic states as resonant states. It was shown that transitions from  $J'' = 2$  sublevel of  $a^5F$  initial state to  $z^5H^0$ ,  $x^5P^0$  and  $y^5G^0$  resonant states are measured. The spectral lines from  $J'' = 3$  sublevel of  $a^5F$  initial state are only observed in  $a^5F_3 \rightarrow y^5G^0$  transition. The transition of these six RLA spectral lines obeyed the select rule of the single photon electronic dipole moment.

The population on excited states has been observed with laser ablation. Such measurement can provide information about the physical process of RLA. It is also known that the high excited states of atom can be selectively populated through resonant multiphoton excitation by RLA. So RLA provides us a suitable way to study the properties of the excited state, such as photo-ionization cross section and lifetime.

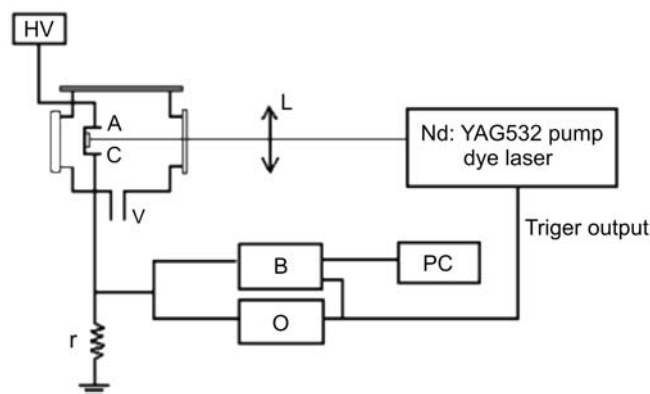


Fig. 1. A schematic of the experimental apparatus: HV – power supply, A – anode, C – cathode, L – lens, B – Boxcar average, O – oscilloscope, PC – computer, r – resistor.

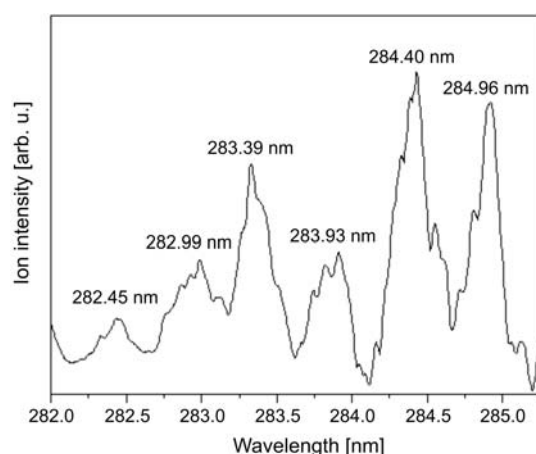


Fig. 2. Resonant laser ablation spectrum of Fe in 281.5–285.5 nm wavelength region.

The relative intensity of four RLA spectral lines ( $a^5F_3 \rightarrow y^5G^0$ ) obtained at the same laser intensity was shown in Fig. 4.

The initial states of these four RLA spectral lines are  $a^5F_2$  and  $a^5F_3$ . The energy value of  $a^5F_2$  state is  $7985.795 \text{ cm}^{-1}$  and for  $a^5F_3$  is  $7728.071 \text{ cm}^{-1}$ . Under local thermodynamic equilibrium (LTE) condition, the atomic population of  $a^5F_2$  state is less than that of  $a^5F_3$ ,

$$N(2) < N(3) \quad (1)$$

where  $N(2)$  is the atomic population of  $a^5F_2$  state and  $N(3)$  is the atomic population of  $a^5F_3$ . According to the theory of laser resonant ionization, we have

$$\frac{dN_i}{dt} = N_1 \sigma_i \Phi \quad (2)$$

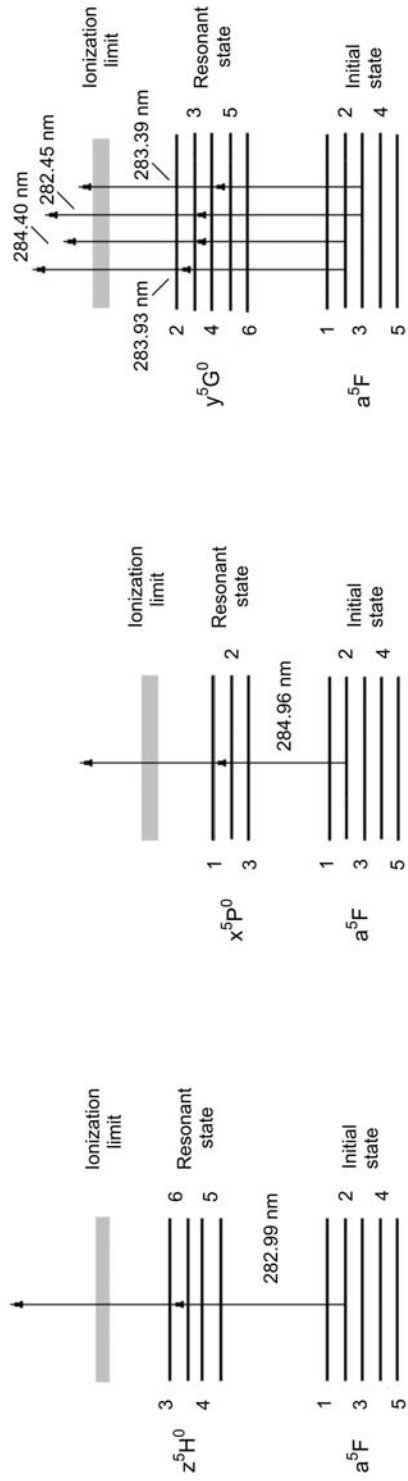


Fig. 3. Energy levels for the scheme of six (1+1) resonant ionization spectral lines of Fe.

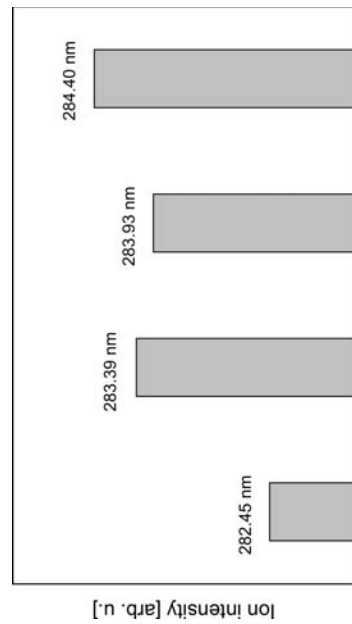


Fig. 4. Relative ion intensity of four RL/A spectral lines produced from  $3d^74s(a^5F) \rightarrow 3d^64s4p(y^5G^0)$  (1+1) resonant-ionization.

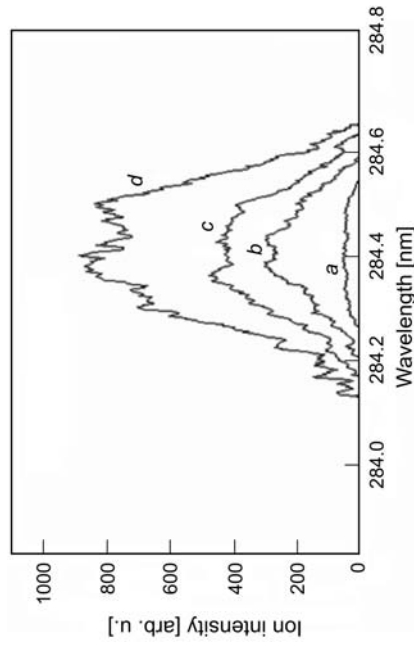


Fig. 5. RL/A spectra of Fe at different laser power densities:  $a = 14$ ,  $b = 29$ ,  $c = 40$ ,  $d = 44$  (unit:  $MW/cm^2$ ).

Equation (2) means that the atoms, which can be ionized, are proportional to the atomic population of the resonant state, the photo-ionization cross section of the resonant state and the laser energy. Under our experimental condition, saturated excitation can be realized, so the atomic population of the resonant state is equal to the atomic population of the initial state,

$$N_1 = N_0 \quad (3)$$

Now the atoms, which can be ionized, are proportional to the atomic population of the initial state, the photo-ionization cross section of the resonant state and the laser energy,

$$N_i \propto N_0 \sigma_i \Phi \quad (4)$$

When the laser energy is a constant, the atoms which can be ionized are proportional to the atomic population of the initial state and the photo-ionization cross section of the resonant state only. According to the relative intensity of these four RLA spectral lines we have

$$N(3)\sigma_{(282.45 \text{ nm})} < N(2)\sigma_{(283.93 \text{ nm})} < N(3)\sigma_{(283.39 \text{ nm})} < N(2)\sigma_{(284.40 \text{ nm})} \quad (5)$$

where  $\sigma_{(282.45 \text{ nm})}$ ,  $\sigma_{(283.39 \text{ nm})}$ ,  $\sigma_{(283.93 \text{ nm})}$  and  $\sigma_{(284.40 \text{ nm})}$  are used to present the photo-ionization cross section of the resonant state, respectively. From Eqs. (1) and (5) we can get the relationship between the photo-ionization cross section of the resonant state and the laser wavelength,

$$\sigma_{(282.45 \text{ nm})} < \sigma_{(283.93 \text{ nm})} < \sigma_{(284.40 \text{ nm})} \quad (6)$$

$$\sigma_{(282.45 \text{ nm})} < \sigma_{(283.39 \text{ nm})} < \sigma_{(284.40 \text{ nm})} \quad (7)$$

It can obviously be seen that there is a proportional relation between the photo-ionization cross section of the resonant state and the laser wavelength.

The effects of laser power density on RLA spectra were presented. The laser power density was varied from the ion detection threshold up to  $10^7 \text{ MW/cm}^2$ . The RLA spectra of Fe at 284.4 nm were shown in Fig. 5. As the laser power density increased, the resonant width of the spectral lines increased symmetrically. The line broadening caused by Stark effect was due to the collision between atoms and charged particles (electrons, ions, *etc.*). An increase in laser power density would lead to an increase in charged particles density in plume and then lead to the line broadening. When the laser power density was below the threshold required for the saturated ionization, the intensity of the spectral lines would be proportional to the laser power density. So the RLA spectra in our experiment were obtained at saturated excitation and unsaturated ionization processes.

The intensity of six spectral lines under different laser power densities ranging from 15 to  $45 \text{ MW/cm}^2$  were shown in Fig. 6. The RLA spectra in our experiment were

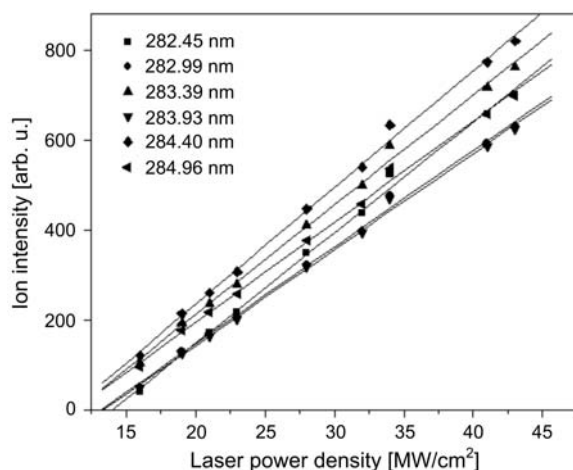


Fig. 6. Effects of laser power density on intensity of six RLA spectral lines laser power densities:  $a = 14$ ,  $b = 29$ ,  $c = 40$ ,  $d = 44$  (unit:  $\text{MW}/\text{cm}^2$ ).

obtained at saturated excitation and unsaturated ionization processes. So, the atoms that can be ionized from the resonant state were proportional to the atomic population of the initial state, the photo-ionization cross section of the resonant state and the laser power density. The possible reasons which might lead to different amplitude increases for different transitions are as follows:

- Different initial state has different atomic population;
- Different resonant state has different photon-ionization cross section;
- The photon-ionization cross section of one electronic state is proportional to the laser wavelength.

#### 4. Conclusions

In this paper, we have presented a comprehensive investigation of resonant laser ablation (RLA) of iron in titanium sample. It is the application of RLA to the analysis of trace analytes within multicomponent sample. Six chosen spectral lines in the region of 281.5 to 285.5 nm are reported for the first time. The initial state of the RLA spectral lines is  $a^5F$ , the resonant states are  $z^5H^0$ ,  $x^5P^0$  and  $y^5G^0$ , respectively. Experiment results show that the photo-ionization cross section of  $y^5G^0$  resonant state is proportional to the laser wavelength. The influence of laser power density on the intensity of RLA spectrum has also been discussed.

#### References

- [1] McLEAN C.J., MARSH J.H., LAND A.P., CLARK A., JENNINGS R., LEDINGHAM K.W.D., MCCOMBES P.T., MARSHALL A., SINGHAL R.P., TOWRIE M., *Resonant laser ablation (RLA)*, International Journal of Mass Spectrometry and Ion Processes **96**(1), 1990, pp. R1–7.

- [2] WANG L., BORTHWICK I.S., JENNINGS R., MCCOMBES P.T., LEDINGHAM K.W.D., SINGHAL R.P., MCLEAN C.J., *Observations and analysis of resonant laser ablation of GaAs*, Applied Physics B: Lasers and Optics **53**(1), 1991, pp. 34–8.
- [3] BORTHWICK I.S., LEDINGHAM K.W.D., SINGHAL R.P., *Resonant laser ablation – a novel surface analytic technique*, Spectrochimica Acta Part B: Atomic Spectroscopy **47**(11), 1992, pp. 1259–65.
- [4] EIDEN G.C., NOGAR N.S., *The two-photon spectrum of iron and silicon detected by resonant laser ablation*, Chemical Physics Letter **226**(5–6), 1994, pp. 509–16.
- [5] LEDINGHAM K.W.D., BORTHWICK I.S., SINGHAL R.P., *The characteristics of resonant laser ablation for surface analysis*, Surface and Interface Analysis **18**(7), 1992, pp. 576–8.
- [6] EIDEN G.C., ANDERSON J.E., NOGAR N.S., *Resonant laser ablation: semiquantitative aspects and threshold effects*, Microchemical Journal **50**(3), 1994, pp. 289–300.
- [7] WANG L., LEDINGHAM K.W.D., MCLEAN C.J., SINGHAL R.P., *Laser-induced collisional processes in resonant laser ablation of GaAs*, Applied Physics B: Photophysics and Laser Chemistry **B54**(1), 1992, pp. 71–5.
- [8] GILL C.G., GARRETT A.W., HEMBERGER P.H., NOGAR N.S., *Selective laser ablation/ionization for ion trap mass spectrometry: resonant laser ablation*, Spectrochimica Acta Part B: Atomic Spectroscopy **51**(8), 1996, pp. 851–62.
- [9] GILL C.G., ALLEN T.M., ANDERSON J.E., TAYLOR T.N., KELLY P.B., NOGAR N.S., *Low-power resonant laser ablation of copper*, Applied Optics **35**(12), 1996, pp. 2069–82.
- [10] BOESL U., *Multiphoton excitation and mass-selective ion detection for neutral and ion spectroscopy*, Journal of Physical Chemistry **95**(8), 1991, pp. 2949–62.
- [11] CONZEMIUS R.J., CAPELLEN J.M., *A review of the applications to solids of the laser ion source in mass spectrometry*, International Journal of Mass Spectrometry and Ion Physics **34**(3–4), 1980, pp. 197–271.
- [12] GIBERT T., DUBREUIL B., BARTHE M.F., DEBRUN J.L., *Investigation of laser sputtering of iron at low fluence using resonance ionization mass spectrometry*, Journal of Applied Physics **74**(5), 1993, pp. 3506–13.

*Received November 9, 2007  
in revised form January 14, 2008*